

## Analog of cosmological particle creation in electromagnetic waveguides

Sascha Lang<sup>1,2,\*</sup> and Ralf Schützhold<sup>1,3,2</sup>

<sup>1</sup>*Helmholtz-Zentrum Dresden-Rossendorf, Bautzner Landstraße 400, 01328 Dresden, Germany*

<sup>2</sup>*Fakultät für Physik, Universität Duisburg-Essen, Lotharstraße 1, 47057 Duisburg, Germany*

<sup>3</sup>*Institut für Theoretische Physik, Technische Universität Dresden, 01602 Dresden, Germany*



(Received 27 May 2019; published 10 September 2019)

We consider an electromagnetic waveguide with a time-dependent propagation speed  $v(t)$  as an analog for cosmological particle creation. In contrast to most previous studies which focus on the number of particles produced, we calculate the corresponding two-point correlation function. For a small steplike variation  $\delta v(t)$ , this correlator displays characteristic signatures of particle pair creation. As another potential advantage, this observable is of first order in the perturbation  $\delta v(t)$ , whereas the particle number is second order in  $\delta v(t)$  and thus more strongly suppressed for small  $\delta v(t)$ .

DOI: [10.1103/PhysRevD.100.065003](https://doi.org/10.1103/PhysRevD.100.065003)

### I. INTRODUCTION

Just a decade after Hubble's discovery of cosmic expansion [1], Schrödinger understood this mechanism to allow for particle creation out of the quantum vacuum [2]. Being one of the most startling predictions of quantum field theory in curved space-times, cosmological particle creation was further studied by Parker [3] and others (see also Ref. [4]) in the late 1960s. In the present Universe, this effect is extremely tiny—but, according to our standard model of cosmology, it played an important role for the creation of seeds of structure formation during cosmic inflation [5]. Signatures of this process can still be observed today in the anisotropies of the cosmic microwave background radiation.

As direct experimental tests of cosmological particle creation are probably out of reach, several laboratory analogs [6–8] for quantum fields in expanding space-times have been proposed for various scenarios, including Bose-Einstein condensates [9–16], ion traps [17–20], and electromagnetic waveguides [21]. In the following, we shall consider the latter system (see also Ref. [22]), which has already been used to observe an analog of the closely related dynamical Casimir effect [21,23–26].

Instead of the often considered number of emerging particles, one can also study other observables, such as the two-point correlation function of the associated quantum field. For condensed-matter analogs of black holes (see, e.g., Refs. [6–8,27]), these correlations have already been studied in several works including Refs. [28–31]. In fact, the observation of analog Hawking radiation in Bose-Einstein condensates reported in Refs. [32] and [33] was based on density correlation measurements.

Cosmological particle creation also generates characteristic signatures in the corresponding field correlations; see also Ref. [14]. Due to spatial homogeneity, particles are created in pairs with opposite momenta. When both particles of a pair arrive at two suitable detectors at different space or space-time points  $(t_1, x_1)$  and  $(t_2, x_2)$ , the associated signals are clearly correlated.

In the following, we study two-point correlations in an electromagnetic waveguide with a time-dependent effective speed of light  $v(t)$ . Reducing this parameter  $v(t)$  effectively increases all length scales in the setup under consideration—in analogy to cosmic expansion. Therefore, laboratory systems with a varying speed of light  $v(t)$  ought to produce photon pairs in close analogy to the mechanism of cosmological particle creation.

### II. CLASSICAL WAVEGUIDE MODEL

Previous research on circuit quantum electrodynamics has brought up various possible implementations of waveguides with tunable parameters; see, e.g., Refs. [21,22,34–36]. Although realistic experiments are often based on superconducting quantum interference devices, they typically still correspond to effective circuit diagrams. In this work, we will focus on waveguide structures that can be modeled with the effective setup illustrated in Fig. 1.

Specifically, we consider an  $LC$  circuit of total length  $D$  which comprises  $N + 1$  capacitors with equal capacities  $C$  and  $N$  inductors with equal but time-dependent inductances  $L(t)$ . Denoting the current in the  $\alpha$ th inductor with the symbol  $I_\alpha$  and the charge on the  $\alpha$ th capacitor with  $Q_\alpha$ , the Lagrangian of the setup from Fig. 1 adopts the form

$$\mathfrak{L}(t) = \sum_{\alpha=1}^{N+1} \frac{1}{2C} Q_\alpha^2(t) - \sum_{\alpha=1}^N \frac{1}{2} L(t) I_\alpha^2(t). \quad (1)$$

\*s.lang@hzdr.de

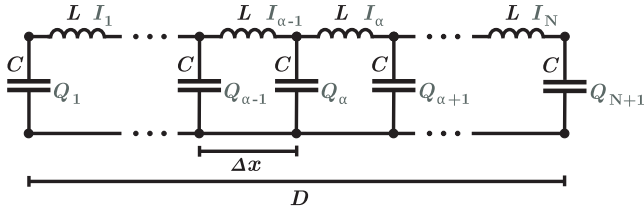


FIG. 1. Illustration of an  $LC$  circuit of length  $D = N\Delta x$  that comprises  $N$  discrete inductors and  $N + 1$  capacitors. The symbols  $I_\alpha$  and  $Q_\alpha$  denote the current in the  $\alpha$ th inductor and the charge on the  $\alpha$ th capacitor, respectively.

Analogous to Ref. [37], we introduce a new generalized flux coordinate  $\Phi_\alpha(t)$  satisfying the relation  $\dot{\Phi}_\alpha(t) = Q_\alpha/\sqrt{C\Delta x}$  and eliminate all currents  $I_\alpha$  in the above Lagrangian  $\mathfrak{L}(t)$  with the second line of the classical Kirchhoff's laws

$$\begin{aligned} \dot{Q}_\alpha &= I_\alpha - I_{\alpha-1}, \\ 0 &= Q_\alpha/C + \partial_t[L(t)I_\alpha] - Q_{\alpha+1}/C. \end{aligned} \quad (2)$$

Apart from this, we describe the discrete setup under consideration in the continuum limit of  $\Delta x \rightarrow 0$  and  $D = \text{const.}$ , which is justified if the length  $\Delta x$  of each mesh in Fig. 1 is significantly smaller than the characteristic wavelengths and the total length  $D = N\Delta x$  of the waveguide [38].

In this limiting case, the charge  $q(t, x) = Q(t, x)/\Delta x$  and current  $j(t, x) = I(t, x)/\Delta x$  per unit length adopt the representations

$$\begin{aligned} q(t, x) &= \left(\frac{C}{L(t)}\right)^{1/4} \frac{1}{\sqrt{v(t)}} \dot{\Phi}(t, x) \\ j(t, x) &= \left(\frac{1}{L^3(t)C}\right)^{1/4} \sqrt{v(t)} \Phi'(t, x), \end{aligned} \quad (3)$$

and the Lagrangian  $\mathfrak{L}(t)$  from Eq. (1) turns into the expression

$$\mathfrak{L}(t) = \frac{1}{2} \int_0^D dx \{ [\dot{\Phi}(t, x)]^2 - v^2(t) [\Phi'(t, x)]^2 \}, \quad (4)$$

where the quantity  $v(t) = \Delta x/\sqrt{L(t)C}$  accounts for the effective speed of light inside the circuit. Throughout this paper, dots are used to denote temporal derivatives  $\dot{\Phi} = \partial\Phi/\partial t$ , while primes indicate spatial derivatives  $\Phi' = \partial\Phi/\partial x$ .

As the waveguide depicted in Fig. 1 is isolated at both ends, the current  $j(t, x)$  vanishes at those points  $x = 0$  and  $x = D$ , resulting in Neumann boundary conditions  $\Phi'(t, 0) = \Phi'(t, D) = 0 \forall t \in \mathbb{R}$  for the generalized flux  $\Phi(t, x)$  [37].

### III. CANONICAL QUANTIZATION

In order to quantize the classical model from above, we follow the path of canonical quantization and obtain the Hamiltonian

$$\hat{\mathfrak{H}}(t) = \frac{1}{2} \int_0^D dx \{ \hat{\Pi}^2(t, x) + v^2(t) [\hat{\Phi}'(t, x)]^2 \} \quad (5)$$

in which the operators  $\hat{\Phi}(t, x)$  and  $\hat{\Pi}(t, x) = \partial_t \hat{\Phi}(t, x)$  satisfy canonical commutation relations for a quantum field and its associated momentum.

The corresponding Heisenberg equations of motion can be combined to the wave equation

$$\ddot{\hat{\Phi}}(t, x) = v^2(t) \hat{\Phi}''(t, x). \quad (6)$$

Bearing in mind that the field  $\hat{\Phi}(t, x)$  has to satisfy Neumann boundary conditions, the mode functions

$$\begin{aligned} \Psi_{n=0}(x) &= \sqrt{1/D} \\ \Psi_{n>0}(x) &= \sqrt{2/D} \cos(\pi n x/D) \end{aligned} \quad (7)$$

allow for a decomposition,

$$\hat{\Phi}(t, x) = \sum_{n=0}^{\infty} \Psi_n(x) \hat{\phi}_n(t), \quad (8)$$

of the field operator  $\hat{\Phi}(t, x)$ , in which each term  $\hat{\phi}_n(t)$  constitutes a harmonic oscillator satisfying the differential equation

$$\ddot{\hat{\phi}}_n(t) = -\omega_n^2(t) \hat{\phi}_n(t) \quad \text{with} \quad \omega_n(t) = \frac{\pi n v(t)}{D}. \quad (9)$$

### IV. SUDDENLY CHANGING SPEED OF LIGHT

#### A. Operator solution for a steplike profile $v(t)$

For a rapidly changing speed of light,

$$v(t) = \begin{cases} v_0, & t < 0 \\ v_1, & t > 0, \end{cases} \quad (10)$$

each operator  $\hat{\phi}_n(t)$  adopts a piecewise representation,

$$\begin{aligned} \hat{\phi}_n(t < 0) &= \frac{1}{\sqrt{2\omega_n^0}} [e^{-i\omega_n^0 t} \hat{a}_n + \text{H.c.}] \\ \hat{\phi}_n(t > 0) &= \frac{1}{\sqrt{2\omega_n^1}} [e^{-i\omega_n^1 t} \hat{b}_n + \text{H.c.}] \end{aligned} \quad (11)$$

with  $\omega_n^i = \pi n v_i/D$ , where the expressions  $\hat{a}_n$  and  $\hat{b}_n$  satisfy canonical commutation relations for two separate sets of bosonic annihilators. The prefactors connecting each operator  $\hat{\phi}_n(t)$  to the corresponding creator and annihilator adopt the same form as for a single harmonic oscillator but

are ill defined in the case of the zero mode  $n = 0$ . This irregularity just corresponds to the standard infrared divergence for massless fields in  $(1 + 1)$  dimensions and has no effect on the corresponding operators  $\hat{q}(t, x) \propto \partial_t \hat{\Phi}(t, x)$  and  $\hat{j}(t, x) \propto \partial_x \hat{\Phi}(t, x)$  for the charge or current because the zero mode is temporally and spatially homogeneous.

The differential equation (9) requires each operator  $\hat{\phi}_n(t)$  and its temporal derivative  $\partial_t \hat{\phi}_n(t)$  to be continuous at  $t = 0$ , which implies the connection

$$\hat{b}_n = \frac{1}{2} \sqrt{\frac{v_1}{v_0}} \left[ \left( 1 - \frac{v_0}{v_1} \right) \hat{a}_n^\dagger + \left( 1 + \frac{v_0}{v_1} \right) \hat{a}_n \right]. \quad (12)$$

### B. Particle creation

Based on the previous relation (12), we can easily study how expectation values for the particle number operator

$$\hat{N}_n(t) = \begin{cases} \hat{a}_n^\dagger \hat{a}_n, & t < 0 \\ \hat{b}_n^\dagger \hat{b}_n, & t > 0 \end{cases} \quad (13)$$

of the  $n$ th mode evolve with time.

In order to demonstrate the occurrence of particle production, we use the Heisenberg picture and study the expectation value  $\langle 0 | \hat{N}_n(t) | 0 \rangle$  for the initial vacuum state  $|0\rangle$ . This state satisfies the relation  $\hat{a}_n |0\rangle = 0$  for all modes  $n$ , because there are no photons inside the waveguide initially. In the regime of  $t > 0$ , the particle number adopts the finite and constant value of  $(v_1 - v_0)^2 / (4v_0v_1)$  for all modes  $n$  (see also Ref. [22]).

Consequently, particle creation for the sudden step  $v(t)$  from Eq. (10) occurs at the sharp instant of  $t = 0$  and uniformly affects all modes [39]. However, the number of particles produced is of second order in the perturbation  $\delta v = v_1 - v_0$ , which might constitute a challenge for future experiments with small  $\delta v$ .

### C. Two-point correlation for the operator $\hat{\Phi}(t, x)$

In case of a sharp step function  $v(t)$ , the two-point correlations for all three operators  $\hat{\Phi}(t, x)$ ,  $\hat{q}(t, x)$ , and  $\hat{j}(t, x)$  can be evaluated analytically. For reasons of clarity, the following considerations will focus on the generalized flux  $\hat{\Phi}(t, x)$ , but corresponding results for the charge  $\hat{q}(t, x)$  and current  $\hat{j}(t, x)$  can easily be obtained (up to a prefactor) by differentiating the expression  $\langle 0 | \hat{\Phi}(t_1, x_1) \hat{\Phi}(t_2, x_2) | 0 \rangle$  with respect to either  $t_1$  and  $t_2$  or  $x_1$  and  $x_2$  [40].

In order to extract real results, we henceforth focus on the expression

$$\kappa(t_1, x_1, t_2, x_2) = \text{Re}[\langle 0 | \hat{\Phi}(t_1, x_1) \hat{\Phi}(t_2, x_2) | 0 \rangle] - \chi_\infty, \quad (14)$$

which has been symmetrized with respect to an exchange of both space-time points  $(t_1, x_1)$  and  $(t_2, x_2)$ . Here, the term  $\chi_\infty$  compensates for the infinite but constant contribution of

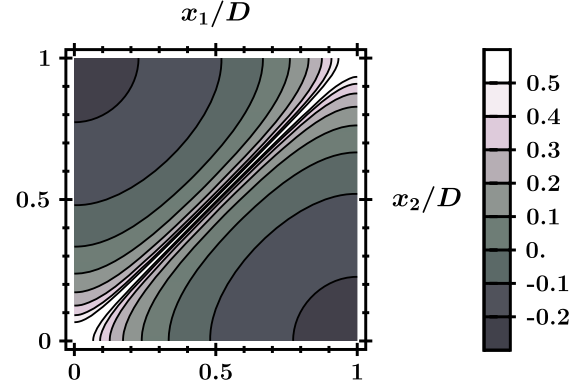


FIG. 2. Rescaled equal-time correlation  $v_0 \kappa(t_1, x_1, t_1, x_2)$  plotted for an arbitrary argument  $t_1 \leq 0$ . Singularities just occur along the line with  $x_1 = x_2$ .

the infrared divergence already discussed in connection with Eq. (11).

Exact analytic results for the correlation  $\kappa(t_1, x_1, t_2, x_2)$  and corresponding expressions for the operators  $\hat{q}(t, x)$  and  $\hat{j}(t, x)$  are calculated in Appendixes A and B. For all pairs of fixed times  $t_1$  and  $t_2$ , the expression  $\kappa(t_1, x_1, t_2, x_2)$  has logarithmic singularities along characteristic lines in the  $(x_1, x_2)$ -plane. The two-point correlations of the other operators  $\hat{q}(t, x)$  and  $\hat{j}(t, x)$  obtained by differentiating  $\kappa(t_1, x_1, t_2, x_2)$  then acquire singularities at the same space-time points, but they are power law  $\propto 1/\xi^2$  instead of logarithmic  $\propto \ln \xi$ , where  $\xi$  is explicitly given in Eq. (A2).

#### 1. Two-point correlation for negative $t_1$ and $t_2$

If both times  $t_1$  and  $t_2$  are negative, the two-point correlation  $\kappa(t_1 \leq 0, x_1, t_2 \leq 0, x_2)$  given in Appendix A diverges to positive infinity under the condition

$$x_1 + s_1 x_2 - s_2 v_0 (t_1 - t_2) = 2Dm \quad (15)$$

with  $s_1, s_2 \in \{\pm 1\}$ , and  $m \in \mathbb{Z}$ .

This identity just accounts for the standard light-cone singularities (including reflections at the boundaries) in the initial vacuum state; see Figs. 2 and 3. For the corresponding charge-charge correlation, condition (15) characterizes divergences to negative infinity. In contrast, divergent contributions to the current-current correlation can have both signs, which results from the fact that the quantity  $j(t, x)$  is phase shifted on each reflection at a boundary with  $j(t, 0) = j(t, D) = 0$  (analogous to a string with fixed ends).

#### 2. Two-point correlation for positive $t_1$ and $t_2$

For positive times  $t_1$  and  $t_2$ , the expression  $\kappa(t_1 > 0, x_1, t_2 > 0, x_2)$  calculated in Appendix A adopts singularities under conditions of two different types:

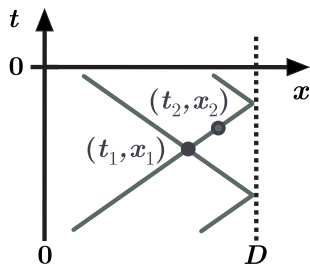


FIG. 3. Worldlines for two different “signals” passing through a given space-time point  $(t_1, x_1)$  at velocities of absolute value  $v_0$ . For all points  $(t_2, x_2)$  on either worldline, the correlation function  $\kappa(t_1 \leq 0, x_1, t_2 \leq 0, x_2)$  diverges.

$$\begin{aligned} x_1 + s_1 x_2 - s_2 v_1 (t_1 - t_2) &= 2Dm \\ x_1 + s_1 x_2 - s_2 v_1 (t_1 + t_2) &= 2Dm. \end{aligned} \quad (16)$$

Except for a modified speed of light, the first identity from Eq. (16) has the same form as the corresponding expression (15) for negative times  $t_1$  and  $t_2$ . It thus also describes usual light-cone singularities.

In contrast, the second type of singularities stems from the creation of particle pairs at  $t = 0$ . As one indication, the second line of Eq. (16) is not invariant under time translation. As another indication, the corresponding prefactors in the result  $\kappa(t_1 > 0, x_1, t_2 > 0, x_2)$  from Appendix A scale linearly with the perturbation  $\delta v = v_1 - v_0$ . In an intuitive picture, one can imagine pair creation at the sharp time  $t = 0$  and some random position  $x_0$ , where the produced particles propagate with opposite velocities  $\pm v_1$ . The condition  $x_2 - x_1 = v_1(t_1 + t_2)$  associated with this configuration is illustrated in Fig. 4.

Figure 5 provides plots of the correlation function  $\kappa(t_1, x_1, t_2, x_2)$  for two fixed pairs of identical positive times  $t_1 = t_2$ . The singularities characterized by the second line of Eq. (16) occur along the black rectangle appearing in both of these plots. As a function of time, the corners of this structure continuously move along the boundaries of the domain  $[0, D]^2$ .

Note that the sign of correlations along the rectangular pattern from Fig. 5 depends on the ratio of both velocities

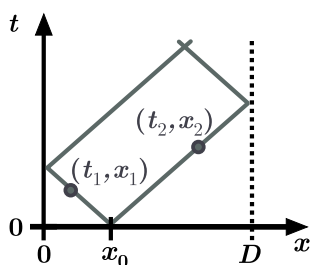


FIG. 4. Worldlines for a photon pair which is produced at an arbitrary position  $x_0$  and the sharp time  $t = 0$ . For all points  $(t_1, x_1)$  and  $(t_2, x_2)$  located on opposite worldlines, the correlation function  $\kappa(t_1 > 0, x_1, t_2 > 0, x_2)$  has singularities characterized by the second line of Eq. (16).

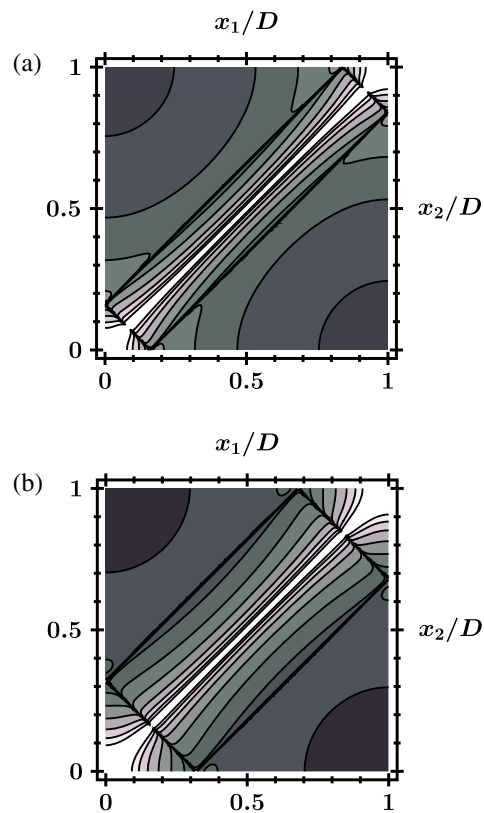


FIG. 5. Rescaled equal-time correlation  $v_0 \kappa(t_1, x_1, t_1, x_2)$  plotted for two different arguments  $t_1 > 0$  and velocities  $v_0 = D$  as well as  $v_1 = 0.8D$ . The parameter  $t_1$  adopts the values 0.1 in plot a) and 0.2 in plot b). Singularities described by the second line of Eq. (16) occur along the black rectangular structure visible in both plots. The color scale is consistent with Fig. 2.

$v_0$  and  $v_1$ . We obtain divergences to negative infinity if  $v_0 > v_1$  and to positive infinity in the case of  $v_0 < v_1$ . Thus, the former case  $v_0 > v_1$  offers the advantage that singularities due to pair production are well distinguishable from light-cone singularities.

The explicit results in Appendixes A and B further reveal that the two-point correlations for both operators  $\hat{\Phi}(t, x)$  and  $\hat{q}(t, x)$  have identical signs along the characteristic rectangle from Fig. 5 but opposite signs under the light-cone condition. Therefore, different types of singularities in the charge-charge correlation can be distinguished by their sign if  $v_0 < v_1$ . As the current alters its sign on reflection at boundaries with  $j(t, 0) = j(t, D) = 0$ , the corresponding correlation can again have both signs depending on the number of reflections involved.

### 3. Two-point correlation for $t_1$ and $t_2$ having opposite signs

If the times  $t_1$  and  $t_2$  differ in sign, we obtain singularities of the same types as in the previous paragraph. Given the exemplary case of  $t_1 < 0$  and  $t_2 > 0$ , divergences occur under the specific conditions

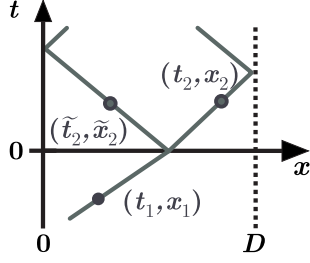


FIG. 6. Two possible worldlines for an initial quantum fluctuation passing through a space-time point  $(t_1, x_1)$  with  $t_1 < 0$ . The condition in the first line of Eq. (17) is satisfied for all points  $(t_2 > 0, x_2)$  that are located on the right branch of the depicted light cone. The second type of singularities emerges for those points  $(\tilde{t}_2 > 0, \tilde{x}_2)$  which belong to the other worldline illustrated above.

$$\begin{aligned} x_1 + s_1 x_2 - s_2(v_0 t_1 - v_1 t_2) &= 2Dm \\ x_1 + s_1 x_2 - s_2(v_0 t_1 + v_1 t_2) &= 2Dm. \end{aligned} \quad (17)$$

Taking the change of propagation velocity at  $t = 0$  into account, singularities specified by the first line of Eq. (17) can be associated with the light cone once again.

On the other hand, the second line of Eq. (17) indicates that quantum vacuum fluctuations propagating at an initial speed of either  $+v_0$  or  $-v_0$  are also partly reflected at the time  $t = 0$  and afterward propagate with the new velocity  $-v_1$  or  $+v_1$ , respectively. An illustration of both possible worldlines emerging from such a partial reflection is provided in Fig. 6. The splitting of initial fluctuations into superpositions of left- and right-moving components corresponds to the mixing of initial creation and annihilation operators  $\hat{a}_n^\dagger$  and  $\hat{a}_n$  in the new annihilators  $\hat{b}_n$  and is hence essential for pair creation. Therefore, the partial reflections encoded in the second line of Eq. (17) also constitute a characteristic imprint of particle production and show how particle creation originates from the initial quantum fluctuations.

## V. CONTINUOUSLY CHANGING SPEED

In order to assess whether the singularities obtained in Sec. IV also arise for smooth profiles  $v(t)$ , we repeat the previous calculations for a continuous function,

$$v^2(t) = \gamma_- \tanh(t/\tau) + \gamma_+ \quad \text{with} \quad \gamma_\pm = \frac{v_1^2 \pm v_0^2}{2}, \quad (18)$$

where  $\tau$  measures the finite time of change.

Particle production in this modified setup can be examined analogous to Sec. 3.4 of Ref. [4] (see also Ref. [41] for technical details). Again, we study the expression  $\kappa(t_1, x_1, t_2, x_2)$  and analyze its behavior along the characteristic lines specified by Eq. (16). This involves several approximations that are further discussed in Appendix C.

### A. Operator solution for a smooth step $v(t)$

For the continuous profile  $v^2(t)$  from Eq. (18), solutions  $\hat{\varphi}_n(t)$  of the differential equation (9) generally have non-trivial time dependencies. However, in the limiting cases of  $t \rightarrow \pm\infty$ , the operators  $\hat{\varphi}_n(t)$  still adopt asymptotic representations equivalent to the expression (11) for a sharp step. Explicit calculations reveal the specific connection

$$\hat{b}_n = \zeta_n^{(+)} \hat{a}_n + \zeta_n^{(-)} \hat{a}_n^\dagger \quad (19)$$

with

$$\zeta_n^{(\pm)} = \sqrt{\frac{\omega_n^1}{\omega_n^0}} \frac{\Gamma[1 \mp i\omega_n^0 \tau] \Gamma[-i\omega_n^1 \tau]}{\omega_n^0 \Gamma[1 \mp \frac{i}{2}(\omega_n^0 \pm \omega_n^1) \tau] \Gamma[\mp \frac{i}{2}(\omega_n^0 \pm \omega_n^1) \tau]} \quad (20)$$

between the asymptotic annihilator  $\hat{b}_n$  after changing the speed of light and the corresponding initial ladder operators  $\hat{a}_n$  and  $\hat{a}_n^\dagger$ ; see also Ref. [4].

### B. Particle creation for a smooth step $v(t)$

By evaluating expectation values  $\langle 0 | \hat{b}_n^\dagger \hat{b}_n | 0 \rangle$  for the initial vacuum  $|0\rangle$ , we find the number of photons created in the  $n$ th mode to adopt the well-known value [4,22]

$$\langle 0 | \hat{b}_n^\dagger \hat{b}_n | 0 \rangle = |\zeta_n^{(-)}|^2 = \frac{\sinh^2[\frac{\pi}{2}(\omega_n^0 - \omega_n^1)\tau]}{\sinh[\pi\omega_n^0\tau] \sinh[\pi\omega_n^1\tau]} \quad (21)$$

for times  $t \rightarrow \infty$  [42]. For sharp step functions with  $\tau \rightarrow 0$  or in the case of  $n = 0$ , the above result reduces to the familiar expression  $(v_0 - v_1)^2 / (4v_0 v_1)$ . On the other hand, the photon number  $\langle 0 | \hat{b}_n^\dagger \hat{b}_n | 0 \rangle$  undergoes exponential decay for  $n \rightarrow \infty$ , which results in a suppression of particle creation at short wavelengths  $\lambda_n = 2D/n$  [44]. Apart from this, particle production also vanishes if the continuous step  $v(t)$  from Eq. (18) has a broad temporal width  $\tau \rightarrow \infty$ .

### C. Two-point correlation after a smooth step $v(t)$

Unlike a sudden step function  $v(t)$ , the continuous profile  $v(t)$  from Eq. (18) does not yield a compact expression for the two-point correlation  $\kappa(t_1, x_1, t_2, x_2)$ . However, for sufficiently large times  $t_1$  and  $t_2 \gg \tau$ , further discussions in Appendix C provide an approximate result  $\kappa(t_1, x_1, t_2, x_2)$  that correctly includes the contributions of modes with large  $n$ . Since all singularities of the quantity  $\kappa(t_1, x_1, t_2, x_2)$  arise from high modes approaching  $n \rightarrow \infty$ , the large- $n$  approximation in Appendix C clearly reveals whether a smooth step  $v(t)$  yields the same divergent contributions as its discontinuous counterpart from Eq. (10) [45].

As expected, we find the two-point correlation  $\kappa(t_1, x_1, t_2, x_2)$  to still diverge under the light-cone conditions

$$x_1 + s_1 x_2 - s_2 v_1 (t_1 - t_2) = 2Dm, \quad (22)$$

while the additional singularities due to pair creation

$$x_1 + s_1 x_2 - s_2 v_1 (t_1 + t_2) = 2Dm \quad (23)$$

from Sec. IV are smoothed for continuous profiles  $v(t)$ . This can be explained by the fact that particle creation can no longer be associated with a sharp point of time.

## VI. CONCLUSION

As a laboratory analog for cosmological particle creation, we have considered a waveguide with a time-dependent speed of light  $v(t)$  and calculated the two-point correlation  $\kappa(t_1, x_1, t_2, x_2)$  for the generalized flux variable  $\hat{\Phi}(t, x)$ . First, we studied a sudden step function  $v(t)$ . In addition to the usual light-cone singularities (including reflections at the boundaries), we found a distinctive pattern of logarithmic singularities in  $\kappa(t_1, x_1, t_2, x_2)$  which clearly reflects the dynamics of pair creation occurring at a sharp instant of time. If we replace the sudden step in  $v(t)$  by a smooth profile, those additional singularities are smoothed. Nevertheless, the correlation  $\kappa(t_1, x_1, t_2, x_2)$  displays distinctive signatures of pair creation, which could be observed experimentally. Qualitatively similar patterns also arise for the two-point correlations of the electric charge  $\hat{q}(t, x)$  and corresponding current  $\hat{j}(t, x)$  inside the waveguide, which might constitute more direct observables.

In contrast to the number of particles produced (see, e.g., Ref. [22]), the imprint of pair creation onto the correlation functions is of first order in the perturbation  $\delta v = v_1 - v_0$ . Therefore, we propose that measuring two-point correlations instead of particle numbers may enhance the chances for observing analog cosmological particle creation in future experiments with tunable waveguides.

## ACKNOWLEDGMENTS

R.S. acknowledges support by German Research Foundation, Grant No. 278162697 (SFB 1242).

## APPENDIX A: CALCULATION OF THE SYMMETRIZED TWO-POINT CORRELATION FOR A RAPID STEP $v(t)$

In order to work out the symmetrized two-point correlation  $\kappa(t_1, x_1, t_2, x_2)$  for a steplike profile  $v(t)$ , we insert the expressions (8) and (11) into Eq. (14). After evaluating all quantum mechanical expectation values, elementary trigonometric identities can be used to rearrange the function  $\kappa(t_1, x_1, t_2, x_2)$  into a sum containing multiple expressions of the characteristic shape

$$\sum_{n=1}^{\infty} \frac{p^n \cos(n\xi)}{n} = -\frac{1}{2} \ln [1 - 2p \cos(\xi) + p^2], \quad p^2 \leq 1, \quad (A1)$$

with here  $p = 1$ , where the result on the right-hand side has been taken from Eq. (1.448) in Ref. [46].

Typical arguments  $\xi$  occurring in terms of the specific shape (A1) can be abbreviated with a symbol

$$\xi_{s_1, s_2}^{(v_i, v_j | \pm)}(t_1, x_1, t_2, x_2) = \frac{\pi}{D} [x_1 + s_1 x_2 - s_2 (v_i t_1 \pm v_j t_2)] \quad (A2)$$

in which the indices  $s_1$  and  $s_2 \in \{\pm 1\}$  constitute placeholders for two variable signs.

By applying the previous considerations to expressions  $\kappa(t_1, x_1, t_2, x_2)$  with different combinations of signs  $\text{sgn}(t_1)$  and  $\text{sgn}(t_2)$ , we obtain the specific results

$$\begin{aligned} \kappa(t_1 \leq 0, x_1, t_2 \leq 0, x_2) &= -\frac{1}{8\pi v_0} \sum_{s_i = \pm 1} \ln [2 - 2 \cos [\xi_{s_1, s_2}^{(v_0, v_0 | -)}(t_1, x_1, t_2, x_2)]] \end{aligned} \quad (A3)$$

$$\begin{aligned} \kappa(t_1 > 0, x_1, t_2 > 0, x_2) &= -\frac{1}{16\pi v_0} \sum_{\gamma = \pm 1} \left[ 1 - \gamma \frac{v_0^2}{v_1^2} \right] \\ &\times \sum_{s_i = \pm 1} \ln [2 - 2 \cos [\xi_{s_1, s_2}^{(v_1, v_1 | \gamma)}(t_1, x_1, t_2, x_2)]] \end{aligned} \quad (A4)$$

and

$$\begin{aligned} \kappa(t_1 \leq 0, x_1, t_2 > 0, x_2) &= -\frac{1}{16\pi v_0} \sum_{\gamma = \pm 1} \left[ 1 - \gamma \frac{v_0}{v_1} \right] \\ &\times \sum_{s_i = \pm 1} \ln [2 - 2 \cos [\xi_{s_1, s_2}^{(v_0, v_1 | \gamma)}(t_1, x_1, t_2, x_2)]] \end{aligned} \quad (A5)$$

For arbitrary fixed arguments  $t_1$  and  $t_2$ , the above findings (A3) to (A5) have logarithmic singularities along characteristic lines in the  $(x_1, x_2)$ -plane. More specifically, such singularities arise if the respective term  $\xi_{s_1, s_2}^{(v_0, v_0 | -)}(t_1, x_1, t_2, x_2)$ ,  $\xi_{s_1, s_2}^{(v_1, v_1 | \gamma)}(t_1, x_1, t_2, x_2)$ , or  $\xi_{s_1, s_2}^{(v_0, v_1 | \gamma)}(t_1, x_1, t_2, x_2)$  corresponds to an integer multiple of  $2\pi$ .

## APPENDIX B: SYMMETRIZED TWO-POINT CORRELATIONS FOR THE CHARGE AND CURRENT IN CASE OF A RAPID STEP $v(t)$

Based on the quantized counterpart of Eq. (3), we can express the symmetrized two-point correlations

$$\begin{aligned} \kappa_q(t_1, x_1, t_2, x_2) &= \text{Re}[\langle 0 | \hat{q}(t_1, x_1) \hat{q}(t_2, x_2) | 0 \rangle] \\ \kappa_j(t_1, x_1, t_2, x_2) &= \text{Re}[\langle 0 | \hat{j}(t_1, x_1) \hat{j}(t_2, x_2) | 0 \rangle] \end{aligned} \quad (B1)$$

for the electric charge  $\hat{q}(t, x)$  and current  $\hat{j}(t, x)$  in terms of the flux-flux correlation  $\kappa(t_1, x_1, t_2, x_2)$  calculated in Appendix A:

$$\begin{aligned}\kappa_q(t_1, x_1, t_2, x_2) &= \left(\frac{1}{L(t_1)L(t_2)}\right)^{1/4} \sqrt{\frac{C}{v(t_1)v(t_2)}} \\ &\quad \times \partial_{t_1} \partial_{t_2} \kappa(t_1, x_1, t_2, x_2) \\ \kappa_j(t_1, x_1, t_2, x_2) &= \left(\frac{1}{L(t_1)L(t_2)}\right)^{3/4} \sqrt{\frac{v(t_1)v(t_2)}{C}} \\ &\quad \times \partial_{x_1} \partial_{x_2} \kappa(t_1, x_1, t_2, x_2).\end{aligned}\quad (\text{B2})$$

Assuming that the sudden step (10) in the speed of light  $v(t)$  is caused by a rapid change of the inductivity  $L(t)$  from initially  $L(t < 0) = L_0$  to the new value  $L(t > 0) = L_1$ , we obtain the following results by inserting the expressions (A3) to (A5) into the function  $\kappa_q(t_1, x_1, t_2, x_2)$  from Eq. (B2):

$$\begin{aligned}\kappa_q(t_1 \leq 0, x_1, t_2 \leq 0, x_2) &= -\frac{\pi}{8D^2} \sqrt{\frac{C}{L_0}} \sum_{s_i=\pm 1} (1 - \cos[\xi_{s_1, s_2}^{(v_0, v_0|^-)}(t_1, x_1, t_2, x_2)])^{-1},\end{aligned}\quad (\text{B3})$$

$$\begin{aligned}\kappa_q(t_1 > 0, x_1, t_2 > 0, x_2) &= -\frac{\pi}{16D^2} \sqrt{\frac{C}{L_1}} \frac{v_1}{v_0} \sum_{\gamma=\pm 1} (-\gamma) \left[1 - \gamma \frac{v_0^2}{v_1^2}\right] \\ &\quad \times \sum_{s_i=\pm 1} (1 - \cos[\xi_{s_1, s_2}^{(v_1, v_1|\gamma)}(t_1, x_1, t_2, x_2)])^{-1}\end{aligned}\quad (\text{B4})$$

and

$$\begin{aligned}\kappa_q(t_1 \leq 0, x_1, t_2 > 0, x_2) &= -\frac{\pi}{16D^2} \left(\frac{C^2}{L_0 L_1}\right)^{1/4} \sqrt{\frac{v_1}{v_0}} \sum_{\gamma=\pm 1} (-\gamma) \left[1 - \gamma \frac{v_0}{v_1}\right] \\ &\quad \times \sum_{s_i=\pm 1} (1 - \cos[\xi_{s_1, s_2}^{(v_0, v_1|\gamma)}(t_1, x_1, t_2, x_2)])^{-1}.\end{aligned}\quad (\text{B5})$$

Due to  $1 - \cos x \geq 0$ , the correlation function  $\kappa_q(t_1 \leq 0, x_1, t_2 \leq 0, x_2)$  before changing the speed of light is negative for all points  $x_1$  and  $x_2$ . In the case of  $v_0 > v_1$ , this statement generalizes to arbitrary combinations of signs  $\text{sgn}(t_1)$  and  $\text{sgn}(t_2)$ . On the other hand, if  $v_0 < v_1$ , all contributions with  $\gamma = 1$  are positive. Analogous to the discussion in Sec. IV, the correlation  $\kappa_q(t_1, x_1, t_2, x_2)$  diverges, wherever the term  $\xi_{s_1, s_2}^{(\dots|\dots)}(t_1, x_1, t_2, x_2)$  equals an even multiple of  $2\pi$ . Singularities with  $\gamma = 1$ , once again, constitute a characteristic signature of particle pair creation.

By considering spatial instead of temporal derivatives of the expressions (A3) to (A5), we obtain similar results,

$$\begin{aligned}\kappa_j(t_1 \leq 0, x_1, t_2 \leq 0, x_2) &= \frac{\pi}{8D^2} \frac{1}{\sqrt{L_0^3 C}} \sum_{s_i=\pm 1} s_1 (1 - \cos[\xi_{s_1, s_2}^{(v_0, v_0|^-)}(t_1, x_1, t_2, x_2)])^{-1},\end{aligned}\quad (\text{B6})$$

$$\begin{aligned}\kappa_j(t_1 > 0, x_1, t_2 > 0, x_2) &= \frac{\pi}{16D^2} \frac{1}{\sqrt{L_1^3 C}} \frac{v_1}{v_0} \sum_{\gamma=\pm 1} \left[1 - \gamma \frac{v_0^2}{v_1^2}\right] \\ &\quad \times \sum_{s_i=\pm 1} s_1 (1 - \cos[\xi_{s_1, s_2}^{(v_1, v_1|\gamma)}(t_1, x_1, t_2, x_2)])^{-1}\end{aligned}\quad (\text{B7})$$

and

$$\begin{aligned}\kappa_j(t_1 \leq 0, x_1, t_2 > 0, x_2) &= \frac{\pi}{16D^2} \left(\frac{1}{L_0^3 L_1^3 C^2}\right)^{1/4} \sqrt{\frac{v_1}{v_0}} \sum_{\gamma=\pm 1} \left[1 - \gamma \frac{v_0}{v_1}\right] \\ &\quad \times \sum_{s_i=\pm 1} s_1 (1 - \cos[\xi_{s_1, s_2}^{(v_0, v_1|\gamma)}(t_1, x_1, t_2, x_2)])^{-1},\end{aligned}\quad (\text{B8})$$

for the correlation of the current  $\hat{j}(t, x)$ . Obviously, these results have the same singularities as the corresponding flux-flux and charge-charge correlations. However, the factor  $s_1$  occurring in the previous expressions allows the correlation  $\kappa_j(t_1, x_1, t_2, x_2)$  to generally adopt either positive or negative values.

### APPENDIX C: APPROXIMATE RESULT FOR THE SYMMETRIZED FLUX-FLUX CORRELATION AFTER A SMOOTH STEP $v(t)$

#### 1. General structure of the two-point correlation for large times $t_1, t_2 \gg \tau$

For times  $t \gg \tau$  located after the smooth step  $v(t)$  from Sec. V, the full quantum field  $\hat{\Phi}(t, x)$  adopts the asymptotic representation

$$\hat{\Phi}(t \gg \tau, x) = \sum_{n=0}^{\infty} \frac{\Psi_n(x)}{\sqrt{2\omega_n^1}} [e^{-i\omega_n^1 t} \hat{b}_n + \text{H.c.}] \quad (\text{C1})$$

in which the terms  $\hat{b}_n$  are given by Eq. (19).

After inserting the above expression into the symmetrized correlation function (14), we obtain (see [42])

$$\kappa(t_1, x_1, t_2, x_2) = \kappa_A(t_1, x_1, t_2, x_2) + \kappa_B(t_1, x_1, t_2, x_2) \quad (\text{C2})$$

with

$$\kappa_A = \sum_{n=1}^{\infty} \frac{1}{2\omega_n^1} \Psi_n(x_1) \Psi_n(x_2) \cos[\omega_n^1(t_1 - t_2)] \\ \times \frac{\sinh^2[\frac{\pi}{2}(\omega_n^0 + \omega_n^1)\tau] + \sinh^2[\frac{\pi}{2}(\omega_n^0 - \omega_n^1)\tau]}{\sinh[\pi\omega_n^0\tau] \sinh[\pi\omega_n^1\tau]} \quad (\text{C3})$$

and

$$\kappa_B = \sum_{n=1}^{\infty} \frac{4\pi}{[(\omega_n^0)^2 - (\omega_n^1)^2]\tau} \Psi_n(x_1) \Psi_n(x_2) \\ \times \text{Re} \left[ \frac{e^{-i\omega_n^1(t_1+t_2)}}{\sinh(\pi\omega_n^0\tau)} \left( \frac{\Gamma[-i\omega_n^1\tau]}{\Gamma[-\frac{i(\omega_n^0+\omega_n^1)\tau}{2}]\Gamma[\frac{i(\omega_n^0-\omega_n^1)\tau}{2}]} \right)^2 \right]. \quad (\text{C4})$$

As the function  $\kappa_A$  just depends on the temporal difference  $t_1 - t_2$ , it corresponds to those terms yielding light-cone singularities in the sudden-step limit of  $\tau \rightarrow 0$ . On the other hand, the expression  $\kappa_B$  is a function of  $t_1 + t_2$  in analogy to the terms from Appendix A which contain an imprint of pair production.

## 2. Expansions allowing for an explicit evaluation

As both expressions  $\kappa_A$  and  $\kappa_B$  involve sums that lack straightforward analytic solutions, the following studies rely on approximations of the respective summands. In order to assess whether the two-point correlation  $\kappa(t_1, x_1, t_2, x_2)$  after a smooth step  $v(t)$  acquires the same singularities as the corresponding expression (A4) for a rapidly changing speed of light, it is sufficient to examine the contributions of modes with large indices  $n \rightarrow \infty$  because using an inaccurate approximation for a finite number of regular summands with low indices  $n$  cannot cause divergence of the entire sum.

Based on the asymptotic expansion

$$\sinh \pi x \sim e^{\pi x}/2 \quad \text{for } x \rightarrow \infty \quad (\text{C5})$$

and the Stirling formula

$$\Gamma(z) \sim \sqrt{2\pi} e^{-z} z^{z-1/2} \quad \text{for } |z| \rightarrow \infty, \quad (\text{C6})$$

we can significantly simplify both expressions (C3) and (C4).

Numerical studies reveal that the relative error associated with the approximation (C5) is negligibly small for all arguments  $x \geq 1$ . Apart from this, the Stirling formula (C6) also yields at least qualitatively reliable results for all purely imaginary arguments  $z = ix$  with  $|x| > 1$ .

Bearing in mind the relation  $\omega_n^i = \pi n v_i / D$ , the expansions (C5) and (C6) are clearly applicable to all summands in the expressions  $\kappa_A$  and  $\kappa_B$  that have sufficiently large indices  $n$ . Moreover, they even hold for smaller integers  $n \gtrsim 1$  if the step width  $\tau$  of the continuous profile  $v(t)$  exceeds the characteristic times  $D/(\pi v_0)$ ,  $D/(\pi v_1)$  and  $2D/|\pi(v_0 - v_1)|$ .

For the exemplary setup studied in Ref. [21], the values  $D = 4$  mm and  $v_0 = 0.5c_0$  constitute realistic experimental

parameters with  $c_0$  denoting the vacuum speed of light. If we further assume  $v_1 = 0.45c_0$ , the asymptotic expansions (C5) and (C6) hold for all indices  $n \in \mathbb{N}$  as long as  $\tau \geq 1.7 \times 10^{-10}$  s.

In the opposite case of  $\tau$  violating the above requirements, the subsequent results contain incorrect contributions for modes with small indices  $n$ . Nevertheless, as explained above, all conclusions concerning the appearance of singularities remain valid even if the underlying approximations are unreliable for low integers  $n$ .

## 3. Approximate result for the term $\kappa_A(t_1, x_1, t_2, x_2)$

By applying the asymptotic expansion (C5) to each summand of Eq. (C3), we obtain the approximate result

$$\kappa_A \approx \sum_{n=1}^{\infty} \frac{\Psi_n(x_1) \Psi_n(x_2)}{2\omega_n^1} \cos[\omega_n^1(t_1 - t_2)] \\ \times [1 + e^{-2\pi \min\{\omega_n^0, \omega_n^1\}\tau}] \quad (\text{C7})$$

that can be further simplified analogous to Appendix A.

More specifically, we expand the square brackets in the last term of Eq. (C7); use the identity (A1) with  $p_1 = 1$  and  $p_2 = \exp[-2\pi^2 \min\{v_0, v_1\}\tau/D]$ ; and finally retain the expression

$$\kappa_A \approx -\frac{1}{8\pi v_1} \sum_{k=1,2} \sum_{s_i=\pm 1} \\ \times \ln [1 - 2p_k \cos[\xi_{s_1, s_2}^{(v_1, v_1)^{-}}(t_1, x_1, t_2, x_2)] + p_k^2]. \quad (\text{C8})$$

The ( $k=1$ ) contribution to the latter result obviously resembles the ( $\gamma = -1$ ) terms in the corresponding function  $\kappa(t_1 > 0, x_1, t_2 > 0, x_2)$  from Appendix A. Therefore, the expression  $\kappa_A(t_1, x_1, t_2, x_2)$  similarly adopts singularities under the condition

$$x_1 + s_1 x_2 - s_2 v_1(t_1 - t_2) = 2Dm. \quad (\text{C9})$$

On the other hand, all terms satisfying  $k=2$  remain finite for arbitrary combinations of space-time points  $(t_1, x_1)$  and  $(t_2, x_2)$ .

## 4. Approximate result for the term $\kappa_B(t_1, x_1, t_2, x_2)$

Based on the Stirling formula (C6), the square brackets in Eq. (C4) can be approximated according to

$$\left( \frac{\Gamma[-i\omega_n^1\tau]}{\Gamma[-\frac{i(\omega_n^0+\omega_n^1)\tau}{2}]\Gamma[\frac{i(\omega_n^0-\omega_n^1)\tau}{2}]} \right)^2 \\ \approx \frac{i\pi\tau(v_0^2 - v_1^2)}{8D v_1} e^{\frac{2\pi^2}{D} n(v_0 - v_1)\Theta(v_0 - v_1)} \\ \times e^{-\frac{i\pi n \tau}{D} [v_0 \ln(\frac{v_0 - v_1}{v_0 + v_1}) + v_1 \ln(\frac{4v_1^2}{|v_0^2 - v_1^2|})]}, \quad (\text{C10})$$

where the symbol  $\Theta$  denotes the Heaviside function.

If we likewise replace the factor  $\sinh(\pi\omega_n^0\tau)$  by means of Eq. (C5), the resulting expression  $\kappa_B$  can be further reduced to the form

$$\kappa_B \approx \sum_{s_j \in \{\pm 1\}} \sum_{n=1}^{\infty} -\frac{s_2}{2\pi v_1} \times \frac{e^{-\frac{\pi^2}{D} \min\{v_0, v_1\}}}{n} \sin[n\tilde{\xi}_{s_1, s_2}(t_1, x_1, t_2, x_2)] \quad (\text{C11})$$

with

$$\begin{aligned} & \tilde{\xi}_{s_1, s_2}(t_1, x_1, t_2, x_2) \\ &= \frac{\pi}{D} [x_1 + s_1 x_2 - s_2 v_1(t_1 + t_2) \\ & \quad - s_2 \tau [(v_0 - v_1) \ln |v_0 - v_1| - (v_0 + v_1) \ln(v_0 + v_1) \\ & \quad + 2v_1 \ln(2v_1)]]. \end{aligned} \quad (\text{C12})$$

By afterward using the identity

$$\sum_{n=1}^{\infty} \frac{p^n \sin(nx)}{n} = \arctan\left(\frac{p \sin x}{1 - p \cos x}\right), \quad p^2 \leq 1, \quad (\text{C13})$$

taken from Eq. (1.448) in Ref. [46], we finally obtain the approximate result

$$\begin{aligned} \kappa_B \approx & \sum_{s_j \in \{\pm 1\}} -\frac{s_2}{2\pi v_1} \\ & \times \arctan\left(\frac{\sin[\tilde{\xi}_{s_1, s_2}(t_1, x_1, t_2, x_2)]}{e^{\frac{\pi^2}{D} \min\{v_0, v_1\}} - \cos[\tilde{\xi}_{s_1, s_2}(t_1, x_1, t_2, x_2)]}\right). \end{aligned} \quad (\text{C14})$$

Since the arctangent adopts finite values for all real arguments, the expression  $\kappa_B$  never diverges. This finding

requires all singularities obeying the second line of Eq. (16) to be smoothened for continuous profiles  $v(t)$ .

### 5. Behavior of former singularities in case of a very broad step $v(t)$

So far, the approximate result  $\kappa_B$  from Eq. (C14) correctly accounts for the contributions of large indices  $n$  only. However, in the limiting case of a broad step  $v(t)$  meeting the requirements  $\tau \gg D/(\pi v_0)$  and  $\tau \gg D/(\pi v_1)$ , i.e., if the speed of light  $v(t)$  changes on timescales greater than the time required by a signal to pass through the entire waveguide, this approximation is valid for all positive integers  $n$ . Nevertheless, inaccurate contributions of small indices  $n$  inevitably become significant for narrow steps  $v(t)$ . Therefore, considerations based on the expression (C14) may yield incorrect results in the sudden-step limit  $\tau \rightarrow 0$ .

For broad steps  $v(t)$  satisfying the relations  $\tau \gg D/(\pi v_0)$  and  $\tau \gg D/(\pi v_1)$ , Eq. (C14) finds the expression  $\kappa_B$  to vanish under the condition  $\tilde{\xi}_{s_1, s_2}(t_1, x_1, t_2, x_2) = m\pi$  with  $m \in \mathbb{Z}$ . If we further assume a weak perturbation  $\delta v = v_1 - v_0$ , the last three terms of Eq. (C12) reduce to a small offset, and the function  $\tilde{\xi}_{s_1, s_2}(t_1, x_1, t_2, x_2)$  hence approaches the corresponding expression  $\xi_{s_1, s_2}^{(v_1, v_1^+)}(t_1, x_1, t_2, x_2)$  from Appendix A. As a result, the function  $\kappa_B$  vanishes under the condition

$$x_1 + s_1 x_2 - s_2 v_1(t_1 + t_2) = Dm, \quad (\text{C15})$$

which includes the lines on which its sudden-step counterpart from Appendix A grows singular.

Although this last observation illustrates how singularities for a rapidly changing speed of light  $v(t)$  are smoothened for very broad steps  $v(t)$ , it does not constitute a quantitative result for the full correlation function  $\kappa(t_1, x_1, t_2, x_2)$  because the term  $\kappa_A$  still has a generally nonvanishing contribution.

- 
- [1] E. Hubble, A relation between distance and radial velocity among extra-galactic nebulae, *Proc. Natl. Acad. Sci. U.S.A.* **15**, 168 (1929).
  - [2] E. Schrödinger, The proper vibrations of the expanding universe, *Physica (Utrecht)* **6**, 899 (1939).
  - [3] L. Parker, Particle Creation in Expanding Universes, *Phys. Rev. Lett.* **21**, 562 (1968).
  - [4] N. D. Birrell and P. C. W. Davies, *Quantum Fields in Curved Space*, Cambridge Monographs on Mathematical Physics (Cambridge University Press, Cambridge, England, 1982).
  - [5] V. F. Mukhanov, H. A. Feldman, and R. H. Brandenberger, Theory of cosmological perturbations, *Phys. Rep.* **215**, 203 (1992).
  - [6] W. G. Unruh, Experimental Black-Hole Evaporation?, *Phys. Rev. Lett.* **46**, 1351 (1981).
  - [7] M. Visser, Acoustic black holes: Horizons, ergospheres and Hawking radiation, *Classical Quantum Gravity* **15**, 1767 (1998).
  - [8] C. Barceló, S. Liberati, and M. Visser, Analogue gravity, *Living Rev. Relativity* **14**, 3 (2011).

- [9] C. Barceló, S. Liberati, and M. Visser, Probing semiclassical analog gravity in Bose-Einstein condensates with widely tunable interactions, *Phys. Rev. A* **68**, 053613 (2003).
- [10] P.O. Fedichev and U.R. Fischer, Gibbons-Hawking Effect in the Sonic de Sitter Space-Time of an Expanding Bose-Einstein-Condensed Gas, *Phys. Rev. Lett.* **91**, 240407 (2003).
- [11] U.R. Fischer, Quasiparticle universes in Bose-Einstein condensates, *Mod. Phys. Lett. A* **19**, 1789 (2004).
- [12] U.R. Fischer and R. Schützhold, Quantum simulation of cosmic inflation in two-component Bose-Einstein condensates, *Phys. Rev. A* **70**, 063615 (2004).
- [13] P. Jain, S. Weinfurter, M. Visser, and C.W. Gardiner, Analog model of a Friedmann-Robertson-Walker universe in Bose-Einstein condensates: Application of the classical field method, *Phys. Rev. A* **76**, 033616 (2007).
- [14] A. Prain, S. Fagnocchi, and S. Liberati, Analogue cosmological particle creation: Quantum correlations in expanding Bose-Einstein condensates, *Phys. Rev. D* **82**, 105018 (2010).
- [15] C. Neuenhahn and F. Marquardt, Quantum simulation of expanding space-time with tunnel-coupled condensates, *New J. Phys.* **17**, 125007 (2015).
- [16] S. Eckel, A. Kumar, T. Jacobson, I. B. Spielman, and G. K. Campbell, A Rapidly Expanding Bose-Einstein Condensate: An Expanding Universe in the Lab, *Phys. Rev. X* **8**, 021021 (2018).
- [17] P.M. Alsing, J.P. Dowling, and G.J. Milburn, Ion Trap Simulations of Quantum Fields in an Expanding Universe, *Phys. Rev. Lett.* **94**, 220401 (2005).
- [18] R. Schützhold, M. Uhlmann, L. Petersen, H. Schmitz, A. Friedenauer, and T. Schätz, Analogue of Cosmological Particle Creation in an Ion Trap, *Phys. Rev. Lett.* **99**, 201301 (2007).
- [19] C. Fey, T. Schaetz, and R. Schützhold, Ion-trap analog of particle creation in cosmology, *Phys. Rev. A* **98**, 033407 (2018).
- [20] M. Wittemer, F. Hakelberg, P. Kiefer, J.-P. Schröder, C. Fey, R. Schützhold, U. Warring, and T. Schaetz, Particle pair creation by inflation of quantum vacuum fluctuations in an ion trap, [arXiv:1903.05523](https://arxiv.org/abs/1903.05523).
- [21] P. Lähteenmäki, G. S. Paroanu, J. Hassel, and P. Hakonen, Dynamical Casimir effect in a Josephson metamaterial, *Proc. Natl. Acad. Sci. U.S.A.* **110**, 4234 (2013).
- [22] Z. Tian, J. Jing, and A. Dragan, Analog cosmological particle generation in a superconducting circuit, *Phys. Rev. D* **95**, 125003 (2017).
- [23] R. Schützhold, G. Plunien, and G. Soff, Trembling cavities in the canonical approach, *Phys. Rev. A* **57**, 2311 (1998).
- [24] J.R. Johansson, G. Johansson, C. M. Wilson, and F. Nori, Dynamical Casimir Effect in a Superconducting Coplanar Waveguide, *Phys. Rev. Lett.* **103**, 147003 (2009).
- [25] J.R. Johansson, G. Johansson, C. M. Wilson, and F. Nori, Dynamical Casimir effect in superconducting microwave circuits, *Phys. Rev. A* **82**, 052509 (2010).
- [26] C. M. Wilson, G. Johansson, A. Pourkabirian, M. Simoen, J. R. Johansson, T. Duty, F. Nori, and P. Delsing, Observation of the dynamical Casimir effect in a superconducting circuit, *Nature (London)* **479**, 376 (2011).
- [27] R. Schützhold and W. G. Unruh, Hawking Radiation in an Electromagnetic Waveguide?, *Phys. Rev. Lett.* **95**, 031301 (2005).
- [28] R. Balbinot, A. Fabbri, S. Fagnocchi, A. Recati, and I. Carusotto, Nonlocal density correlations as a signature of Hawking radiation from acoustic black holes, *Phys. Rev. A* **78**, 021603 (2008).
- [29] I. Carusotto, S. Fagnocchi, A. Recati, R. Balbinot, and A. Fabbri, Numerical observation of Hawking radiation from acoustic black holes in atomic Bose-Einstein condensates, *New J. Phys.* **10**, 103001 (2008).
- [30] J. Macher and R. Parentani, Black-hole radiation in Bose-Einstein condensates, *Phys. Rev. A* **80**, 043601 (2009).
- [31] R. Schützhold and W. G. Unruh, Quantum correlations across the black hole horizon, *Phys. Rev. D* **81**, 124033 (2010).
- [32] J. Steinhauer, Observation of quantum Hawking radiation and its entanglement in an analogue black hole, *Nat. Phys.* **12**, 959 (2016).
- [33] J.R.M. de Nova, K. Golubkov, V.I. Kolobov, and J. Steinhauer, Observation of thermal Hawking radiation and its temperature in an analogue black hole, *Nature (London)* **569**, 688 (2019).
- [34] P.D. Nation, M.P. Blencowe, A.J. Rimberg, and E. Buks, Analogue Hawking Radiation in a dc-SQUID Array Transmission Line, *Phys. Rev. Lett.* **103**, 087004 (2009).
- [35] M. A. Castellanos-Beltran, K. D. Irwin, G. C. Hilton, L. R. Vale, and K. W. Lehnert, Amplification and squeezing of quantum noise with a tunable Josephson metamaterial, *Nat. Phys.* **4**, 929 (2008).
- [36] P. Navez, A. Sowa, and A. Zagoskin, Entangling continuous variables with a qubit array, [arXiv:1903.06285](https://arxiv.org/abs/1903.06285).
- [37] See Supplemental Material of Ref. [21] at [www.pnas.org/content/suppl/2013/02/12/1212705110.DCSupplemental](http://www.pnas.org/content/suppl/2013/02/12/1212705110.DCSupplemental).
- [38] Note that later calculations for a sharp step function  $v(t)$  actually predict the creation of photons with arbitrary wavelengths  $\lambda_n = 2D/n$ ,  $n \in \mathbb{N}$ . However, similar considerations for smoother profiles  $v(t)$  suggest that particle production at large wave numbers  $n$  is suppressed in real experiments [4]. Therefore, using the continuum limit is reasonably justified at least for the experimentally relevant modes satisfying  $\lambda_n \gg \Delta x$ .
- [39] This finding implies the generation of photons even in modes with arbitrarily high  $n$ . However, as already pointed out in [38], this finding just holds for sharp steplike profiles  $v(t)$  and does not apply to more realistic setups with smoother parameter changes.
- [40] Which physical quantity is the most promising observable in analog studies of cosmological phenomena depends on the specific setup under consideration. In experiments with Bose-Einstein condensates (see, e.g., Refs. [32,33]), one typically studies densities corresponding to canonical momenta rather than the actual phase field.
- [41] F. Sauter, Zum ‘Kleinschen Paradoxon’, *Z. Phys.* **73**, 547 (1932).
- [42] The underlying calculations are based on the two identities  $|\Gamma(iy)|^2 = \pi/[y \sinh(\pi y)]$  and  $|\Gamma(1+iy)|^2 = \pi y/\sinh(\pi y)$  from Eqs. (6.1.29) and (6.1.31) in Ref. [43].

- [43] M. Abramowitz and I. A. Stegun, *Handbook of Mathematical Functions* (National Bureau of Standards, Washington, D.C., 1964).
- [44] This finding resolves the issue raised in [38].
- [45] Even if the underlying approximations do not hold for small indices  $n$ , the total error in the full correlation function essentially stems from a finite number of regular summands and hence has to be finite.
- [46] I. S. Gradshteyn and I. M. Ryzhik, *Table of Integrals, Series and Products*, 8th ed. (Academic Press, New York, 2015).